Bull Volcanol (2014) 76:843
DOI 10.1007/s00445-014-0843-5

RESEARCH ARTICLE

Relatively short-term correlation among deformation, degassing, and seismicity: a case study from Concepción volcano, Nicaragua

José Armando Saballos · Vladimir Conde · Rocco Malservisi · Charles B. Connor · Julio Álvarez · Angélica Muñoz

Received: 29 July 2013 / Accepted: 15 June 2014

Abstract Concepción is a frequently active composite volcano in Nicaragua, and is located on Ometepe Island, within Lake Nicaragua. Significant eruptive activity took place at this volcano between March and May 2010, consisting of ash and gas explosions (VEI 1–2). We compare geodetic baseline changes observed with global positioning system (GPS), sulfur dioxide flux (SO_2), and seismic amplitude (SAM) data collected at Concepción during April – June, 2010, and February – April, 2011. Time series analysis reveals a remarkable correlation among the data sets during 2010, when the volcano was erupting. In contrast, the volcano was at its background level of activity in 2011 and the statistical correlation among the time series is not significant for this period. We explain the emergence of correlation among the time series during eruptive activity through modeling of the GPS data with emplacement of a magma column in an open conduit. In the model, magma rose in the conduit, between May 5 and 14, 2010, from a shallow reservoir located at ∼1.8 km depth. Later, between May 24 and 31, 2010, the top of the magma column descended to almost 600 m depth, corresponding to the cessation of eruptive activity. Thus, cross-correlation and an integrated analysis of these geophysical time series on a timescale of days helps to reveal the dynamics of the magma plumbing system operating below Concepción volcano.

Keywords Volcano deformation · GPS · SO2 · Flux · Seismic amplitude measurement · Time series · Open conduit · Concepción volcano

Editorial responsibility: S. De la Cruz-Reyna

Electronic supplementary material The online version of this article (doi:10.1007/s00445-014-0843-5) contains supplementary material, which is available to authorized users.

J. A. Saballos (✉) · J. Álvarez · A. Muñoz
Instituto Nicaragüense de Estudios Territoriales, Apdo. postal 2110, Managua, Nicaragua
e-mail: j.a.saballos@gmail.com

J. Álvarez
e-mail: julio.alvarez@gf.ineter.gob.ni

A. Muñoz
e-mail: angelica.munoz@gf.ineter.gob.ni

V. Conde
Chalmers University of Technology, Earth and Space Sciences, SE-412 96 Göteborg, Sweden
e-mail: conde@chalmers.se

R. Malservisi · C. B. Connor
School of Geosciences, University of South Florida, 4202 E. Fowler Ave., Tampa, FL 33620, USA

R. Malservisi
e-mail: rocco@usf.edu

C. B. Connor
e-mail: cbconnor@usf.edu

Introduction

During volcanic activity of 2010, surface deformation around Concepción volcano, Nicaragua, was characterized by semi-periodic changes in baseline lengths measured across the volcano of up to ∼4 cm with period of several days to weeks. Modeling the source of this deformation may lead to improved understanding of how conduit processes govern eruption frequency and intensity in open magma systems, like Concepción (e.g., van Wyk de Vries 1993; Borgia and van Wyk de Vries 2003; Saballos 2013; Saballos et al. 2013). Insight into the open conduit model can be gained by cross-correlating time series of global positioning system (GPS) measurements, average seismic amplitude measurements (SAM), and SO_2 flux data.

Joint interpretation of surface deformation, SO_2 flux, and seismic data for periods of weeks to months provides a more integral view of volcanic processes than the analysis of any single data set (Casadevall et al. 1981; McGee and Sutton 1994; Voight et al. 1999; Watson et al. 2000; Williams-Jones et al. 2001; Olmos et al. 2007). With new advances in instrumentation, it has become routine to gather multivariable measurements at high sampling rates (up to 1 Hz, or even higher), allowing the study of short-term variations (seconds to hours) of the dynamics of magmatic systems associated with individual eruptions or episodes of volcano unrest (Fischer et al. 2002; Gottsmann et al. 2007; Dalton et al. 2010; Kazahaya et al. 2011; Nadeau et al. 2011; Ichihara et al. 2012). In this study, we show that the comparison of daily observations of GPS geodetic measurements, SAM, and SO_2 flux of intermediate length (~2 month sampling period during 2010) also exhibit highly correlated behavior during one eruptive period at Concepción volcano. In contrast, during a non-eruptive period (~2.5 month sampling period during 2011) of this volcano, significant cross-correlations among these variables are not present. We suggest that the correlation among different data sets provides important insights into volcanic processes on timescales of days to weeks during unrest at Concepción volcano. We develop our model to attempt to explain magma movement on these timescales.

Changes in baseline length, SAM, and SO_2 flux were not of particularly large magnitude during the eruptive phase compared to the non-eruptive phase, although anomalous behavior is observed in all three times series during the eruption, these anomalies become most clear by cross-correlating the time series. This result is perhaps not surprising for an open-vent volcano. However, this observation reinforces the idea that a continuous monitoring program of several geophysical time series, and near-real time cross-correlation of these time series, might improve future responses to eruptive crises at Concepción and possibly other open vent volcanoes.

Concepción volcano

Concepción is currently the most active composite volcano in Nicaragua (the most active one is Cerro Negro) volcano, a small and young cinder cone (e.g., Hill et al. 1998) and is predominantly composed of clinopyroxene–plagioclase bearing andesite rocks (McBirney and Williams 1965; van Wyk de Vries 1993; Borgia et al. 2003). During the last four decades, volcanic activity at Concepción has been characterized by small to moderate explosions (VEI 1-2) of tephra and gas (van Wyk de Vries 1993; Borgia et al. 2003; Siebert et al. 2011). We note, however, that eruptive activity at Concepción has not always been so mild. Plinian and sub-Plinian tephra fallout deposits are found in the late Pleistocene and Holocene stratigraphic records (McBirney and Williams 1965; Borgia et al. 2003; Kutterolf et al. 2008). Furthermore, past effusive eruptive activity has produced voluminous flank lava flows. The greatest concern for a large eruption of Concepción lies in the effective evacuation of the island's ~31,000 inhabitants (INIFOM 2001). In addition to hazards directly related to the volcanic activity, hazards associated with the remobilization of tephra fallout as lahars during subsequent rainfall are of great concern. These lahars, although small in volume, have damaged infrastructure and inundated agricultural areas (INETER 2008).

The eruption of 2010

According to reports from the Instituto Nicaragüense de Estudios Territoriales (INETER), a new eruptive phase consisting of ash- and gas- laden explosions that rose up to 1 km above the crater began on March 7, 2010 (INETER 2010b). From March 8 to March 17, INETER personnel observed and counted the number of visible ash and gas explosions that occurred during daylight. They registered an average of 30 explosions per day, with a minimum of 14 explosions per day on March 8, and a maximum of 43 explosions per day on March 13 (INETER 2010b). Fewer daily explosions were observed through March 24, then explosions became much more sporadic and the volcano was less regularly observed (INETER 2010b). The Washington Volcanic Ash Advisory Center issued five reports of volcanic ash from Concepción volcano detected by satellite. Two reports were issued on March 8 followed by single reports on March 9, 12, and 13, 2010 (http://www.ssd.noaa.gov/VAAC/ARCH10/archive.html#CONC).

Reports from INETER mention that ash explosions continued until mid-April (INETER 2010a), and island residents reported eruptive activity until mid-May, 2010. We observed low intensity (VEI 1) explosions during April 1 and 15 that deposited a very fine ash layer (< 1 mm thick) on the volcano's WSW flank and in nearby communities. In general, during this period, eruptions were characterized by an initial explosion, quickly followed by two or three additional explosions of smaller intensity at irregular time intervals. At the time of writing (March 2014), no new unrest has been reported from Concepción volcano since mid-May, 2010.

Average seismic tremor frequency at Concepción rose from a background of 0.5 Hz before March 7, 2010 to an average frequency of ~3 Hz in the following 2 weeks. SAM maximum daily average, 94 units, occurred on March 20 (INETER 2010b). During the same period, INETER staff made mobile SO_2 measurements with a Differential Optical Absorption Spectrometer, DOAS (e.g., Galle et al. 2003), along the main road on the N and W side of Concepción volcano obtaining SO_2 daily fluxes averages on March 9 and March 13 – 15 of 133, 91, 507, and 127 tons/day, respectively (INETER 2010b).

Data collection and analysis

Geodetic GPS data

We collected dual-frequency GPS data at two sites simultaneously during April 8 – June 25, 2010, and February 4 – April 16, 2011. These sites are located on the northern (CON1) and southeastern (SINT) flanks of Concepción volcano. Data collected at these two sites were used to compute a daily geodetic baseline across the northeastern side of the volcano (Fig. 1).

GPS data were processed using the Jet Propulsion Laboratory (JPL)'s software GIPSY-OASIS 6.1.2 to produce non-fiducial daily solutions, following the procedure described in Saballos et al. (2013). The final product of the processing consists of time series of the three components (E–W, N–S, and up–down) of the daily position for each site with respect to the International Terrestrial Reference Frame of 2008 (Altamimi et al. 2011). Daily baseline length computation between CON1 and SINT sites (Fig. 2) was also performed with the GIPSY-OASIS software. During the full period, the average distance of the two sites was 5,915.765 m with a daily formal error of the order of 3 mm.

Average seismic amplitude (SAM) data

SAM data were collected using a broadband seismometer co-located with the CON1 GPS site. SAM counts consist of the average of the absolute seismic signal's amplitude calculated at a ten minute interval (Endo and Murray 1991), which we averaged over a 24 h interval to get SAM daily counts. In early 2011, a new seismic instrument was set-up with a different gain setting at CON1 site (V. Tenorio, personal communication, 2011) producing a background level reading about ten times larger than the 2010 counts. To better compare the SAM 2010 and 2011 time series, we divided the most recent SAM counts by ten. This step does not affect the cross-correlation of the SAM data with the other variables in any way.

Remotely-sensed SO_2 data

SO_2 measurements were made by the Differential Optical Absorption Spectroscopy, DOAS, technique (Platt and Stutz 2008) using ground–fixed instruments developed under the Network for Observation of Volcanic and Atmospheric Change, NOVAC, project (Galle et al. 2010). One mini-DOAS instrument was installed in late April 2010 at a site ~6 km southwest of the volcano's crater (Japón, Fig. 1). A second instrument was installed in March 2011 ~2.5 km west of the volcano's crater (Morro, Fig. 1). The instrument setup and data acquisition procedure are the same as that described by Galle et al. (2010). Given the characteristics of the plume from Concepción (it predominantly bends over after leaving the volcano's crater), the plume height is assumed to be the same as the volcano's height (1,600 m a.s.l). The plume speed is assumed to be the same as the wind speed at the volcano's height and was obtained from the Global Forecast System models data from the National Ocean and Atmospheric Administration. The mini-DOAS instruments run during daylight; typically from 6:00 to 18:00 local time (GMT-6, thus within a single 24-h GPS day). To be consistent with the temporal resolution of GPS data, we averaged the observations to daily fluxes. The SO_2 data were post-processed using the algorithm described by Platt and Stutz (2008).

Data gaps

In order to compute cross-correlation and periodograms, gaps in the data (days on which no measurements were obtained) were filled using the nearest neighbor, cubic splines, or piecewise cubic Hermite interpolation methods, depending on which interpolation method produced the closest variance to the original data set. For the 2010 period, there are no GPS data gaps. In 2011, there were five missing days (February 16, March 13, March 31, April 3, and April 13, open circles in Fig. 2) mainly related to missing GPS epochs in the daily data file due to power supply failure. SAM time series contain three missing days in 2010 (April 11, and May 10 and 11) and none in 2011. Gaps in the SAM data were mainly related to problems with the telemetry system (V. Tenorio, personal communication, 2011).

The 2010 SO_2 data have gaps on April 30, and May 1, 8, 9, and 24 to 26. One gap occurred in 2011 (April 7). Gaps in the SO_2 data were due to failure to detect the gas plume (i.e., clouds between the instruments and the volcanic plume were too dense) and/or to failure of the automatic instruments to resolve the plume geometry, a required parameter to compute the SO_2 flux. During 2010, only one mini-DOAS instrument was in operation, whereas two were in operation during 2011. This fact accounts for the larger number of missing days in the SO_2 data during 2010, as opposed to only one missing day in the time series in 2011. We tested the effects caused by the data interpolation and gaps on the cross-correlations (see Discussion and conclusions section), and found the cross-correlation of variables is not sensitive to the interpolation method.

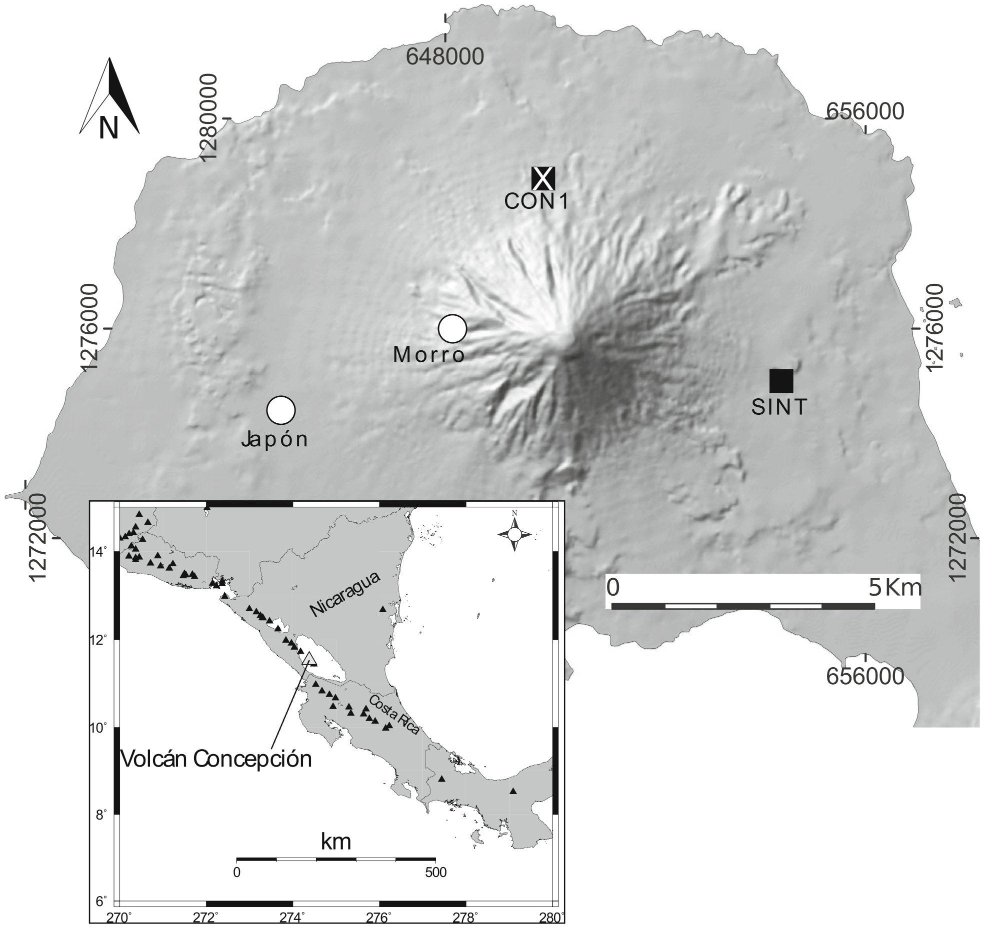

Fig. 1 Shaded relief map of Concepción volcano. *Black squares* depict the location of the dual-frequency GPS sites. The *white "X"* on the black square at CON1 shows the location of the only continuously operating seismic station at Concepción. *White circles* show the location of the SO_2 mini-DOAS instruments. Inset: Regional location map of Concepción volcano, Nicaragua, in Central America. *Black triangles show* the location of major Quaternary volcanoes along the Central America volcanic front

Results

Three time series corresponding to each data type were correlated for GPS baseline, SAM, and SO_2 flux during 2010 (April 8 through June 25 for GPS and SAM cross-correlation, and April 28 through June 24 for SO_2 with the GPS and SAM data sets, Fig. 2) and 2011 (February 4 through April 16). Time series for 2010 period were collected during the final phase of the eruptive activity.

For 2010, the maximum change in GPS geodetic baseline length between CON1 and SINT sites (Fig. 1) has a total amplitude of 29 mm (-16 to 13 mm). This variation appears to be time-correlated and occurs progressively over periods of days to weeks, resulting in the broad fluctuations about the mean baseline length (0 mm, Fig. 2a). The maximum GPS baseline change took place on May 14, 2010, 4 days after island residents reported an explosion, the last explosion reported during the 2010 activity. On May 16, the baseline length returned to its average value, as does the SAM (71 SAM units), while the SO_2 was slightly above its mean value (266 tons/day; Fig. 2a). The pattern of variation of GPS and SAM is very similar with a sharp increase between May 5 and 14, and a sharp decrease in the GPS data between May 24 and 31, 2010, and a coeval increase in the SAM signal (Fig. 2a). The SO_2 emissions began to increase on May 5 and reach a maximum (643 tons/day, or 7.44 kg/s) on May 10, the day of the last reported explosion, then fall to background levels (~200 tons/day) around May 17. Anomalously high values for change in baseline length, SAM, and SO_2 emissions occur within a time window between May 5 and 14, and are nearly in phase.

On May 24 – 27, 2010, the GPS baseline contracts, then returns to average length by May 31 (Fig. 2a). SAM is elevated during this period, while the SO_2 emissions remained at near average values (Fig. 2a).

Overall, the daily average of SO_2 flux appears to correlate positively with positive changes in GPS baseline length. Fluxes >300 tons/day all correspond to positive changes (extension) in GPS baseline (Fig. 2a). A similar pattern is revealed by comparing SO_2 and SAM in that all SO_2 fluxes >300 tons/day occur when daily SAM values were >77 units. Unfortunately, the seismic waveform data in the INETER archive are lost for this and other time periods (V. Tenorio, personal communication, 2014), and seismic analysis must be restricted to changes in SAM values reported in INETER's monthly bulletins.

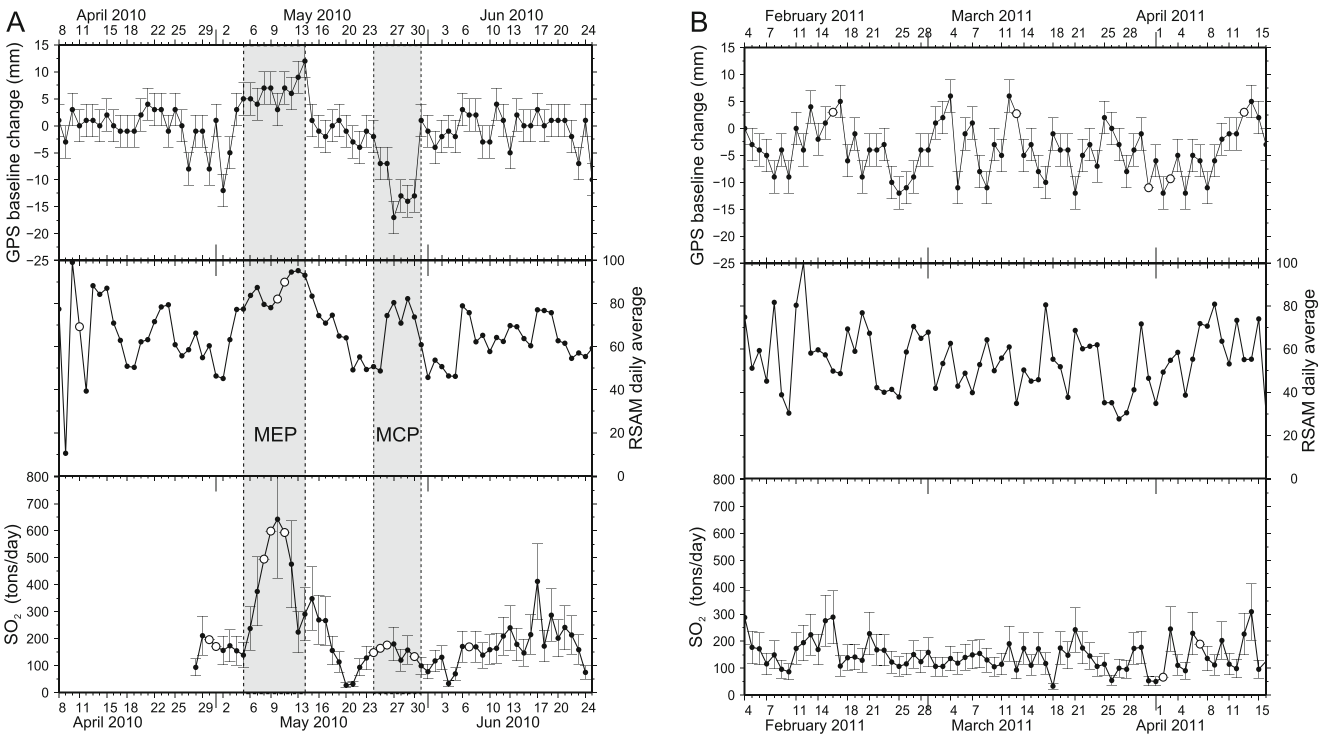

Fig. 2 Time series of the 2010 and 2011 data used in this study. MEP stands for major extension phase in the GPS signal, while MCP major contraction phase shown in the GPS data. GPS baseline daily changes with regard to the first day on the time series. *Error bars* reflect formal error computed for a full observation day composed of measurements every 30 s. SAM daily average of measurements every 10 min. SO_2 daily fluxes. *Error bars* represent 34 % uncertainty of the observed value for a full day composed of varying number of measurements, 5 per day in average, and up to 35 measurements maximum. *Closed circles* represent observed data, while *open circles* interpolated data. The interpolation method that yielded the best results for the GPS time series during the 2010 and 2011 period was the Piecewise Cubic Hermite. For the SO_2 during 2010, the interpolation method was the Nearest Neighborhood and the Cubic Spline during 2011. In the case of the SAM data, the Cubic Spline and the Piecewise Cubic Hermite gave the same results. **a** 2010 period when the volcano was in its most recent eruptive phase that begun on March 7 and extended up to around the end of May. **b** The 2011 data correspond a period when the volcano was not erupting

These relationships between SO_2 and GPS, and SO_2 and SAM present during the eruptive phase of 2010 are not present during the 2011 time series data (Fig. 2b). The maximum amplitude in GPS baseline change during the 2011 data set was 18 mm (-12 to 6 mm), which is 11 mm less than the 2010 counterpart (Fig. 2a) and is characterized by random variation about the mean, as opposed to the smoother variations observed during the eruptive phase in 2010. In a similar way, the SAM data collected in 2011 are characterized by random variation about the mean. During the 2011 time series, the maximum daily average of SO_2 fluxes is 52 % smaller (maximum daily flux was 309 tons/day or 3.58 kg/s, Fig. 2b) than the maximum observed values during eruptive activity in 2010.

Additional structure in the time series is revealed by computing their periodograms (Fig. 3a–c). Significant autocorrelation exists in all three times series collected during the eruptive episode in 2010. The relatively broad spectrum of each series confirms our previous qualitative interpretation that signal is found in the time series during the eruptive period, and the decay observed in the amplitude of this periodogram at longer periods indicates a significant autocorrelation of each time series on time scales of 3–10 days (Fig. 3). In contrast, the periodograms for the time series collected during the non-eruptive period of 2011 are structureless and characterized by uniform low amplitude at each period (Fig. 3). That is, variation in GPS baseline length, SAM, and SO_2 emissions is time-correlated within windows of several days to ∼1 week during the eruptive period of 2010, while the data are non-time correlated and random for the non-eruptive period of 2011.

Cross-correlograms provide further insight into the structure of the time series during the 2010 eruption and the 2011 non-eruptive period. The 2010 time series are characterized by correlation coefficients that are significantly different from zero (Fig. 4a, c, e), whereas the 2011 non-eruptive period shows poor or no correlation, except at lags 0 and 1 (Fig. 4b, d, f). In other words, the time series collected during the non-eruptive period of 2011 present only a slight correlation between two observables (e.g., GPS baselines and SAM) on any single day, but this correlation does not extend to subsequent days (Fig. 4b, d, f). On the other

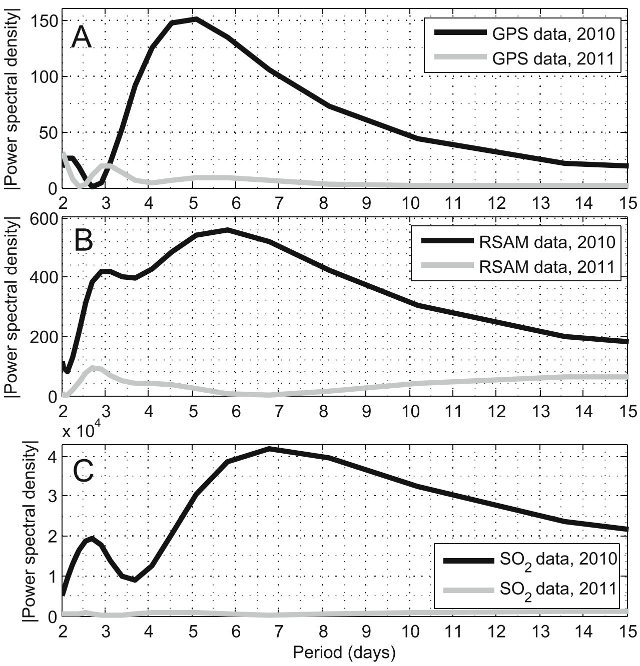

Fig. 3 Periodograms were smoothed by a Hanning window (e.g., Chatfield 1996). **a** The 2010 GPS time series has significant autocorrelation with a maximum at about 5-day period. **b** The 2010 SAM data and **c** 2010 SO_2 reveal similar broad autocorrelation with a maximum between 5 and 7 days. The periodograms of the 2011 data sets uniformity low amplitude power spectra compared to their 2010 counterparts, thus they do not have any meaningful autocorrelation and are best characterized by random fluctuation around mean values

hand, during the 2010 eruptive period, significant cross-correlation between different observables persist to lag of approximately ±5 days (Fig. 4a, c, e).

The largest correlation coefficients are observed between 2010 GPS baseline and SO_2 emission at lag -3 days (Fig. 4c) and SO_2 emission and SAM at lag zero days (Fig. 4e). The maximum correlation coefficient at -3 days suggests that during the 2010 eruptive period GPS baseline changes have a tendency to lead changes in SO_2 emission, although this tendency is quite subtle and may not be significant.

Modeling

During the March to May 2010 eruptive phase of Concepción volcano, the GPS baseline lengthens when the volcano was erupting ash and gases, and contracts when the explosions ceased (Fig. 2a). These changes in GPS baseline length were accompanied by subtle but significant changes in SAM and SO_2 emission. An important feature of the observed changes in the GPS baseline is that the average change returns to zero after these short-term (a few days long) extension and contraction phases, implying that the volcano experienced a recoverable (elastic) deformation. Thus, we interpret GPS baseline extension as inflation of the volcano edifice (May 5 – 13, 2010; Fig. 2), and baseline contraction as deflation (May 23 – 29, 2010; Fig. 2), compared to average conditions. This type of surface deformation has been observed during small to moderate eruptions at other volcanoes, such as Mount Etna, Mount Saint Helens, Merapi, Montserrat, Unzen, and others (Bonaccorso and Davis 1999; Nishimura 2009 and references therein).

A simple model that can explain this kind of volcano edifice variation is one of deformation induced by a cylindrical column of magma rising from a shallow magma reservoir

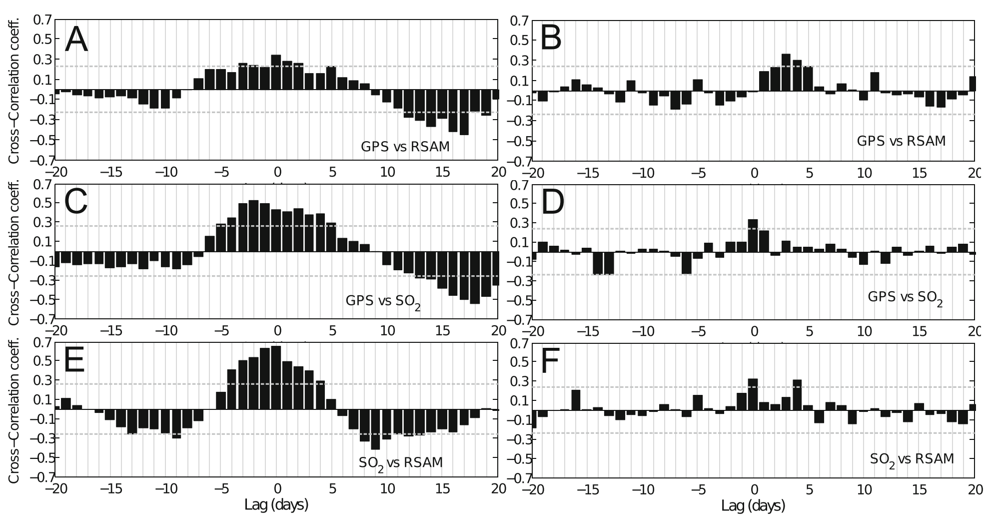

Fig. 4 Cross-Correlograms among all time series. *Dashed horizontal gray lines* represent the 95 % confidence interval, above or below which the correlation is statistically significant ($\pm 2/\sqrt{N}$, where N is the number of observed points). **a** Cross-correlogram between the GPS and SAM data for 2010. Positive correlation at positive lags means SAM leads GPS baseline changes; positive correlation at negative lags means GPS baseline leads SAM changes. **b** Cross-correlegram between the GPS and SAM data for 2011; **c** CGPS and SO_2 data for 2010; **d** GPS and SO_2 data for 2011; **e** SO_2 and SAM data for 2010; **f** SO_2 and SAM data for 2011

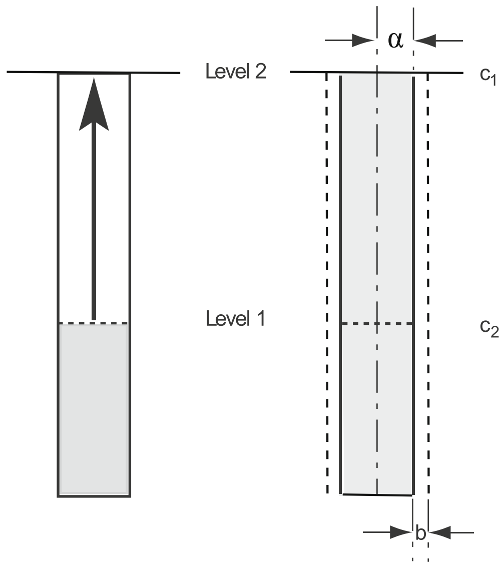

Fig. 5 Schematic representation of the open pipe model, after Bonaccorso and Davis (1999), that we use to model the geodetic GPS deformation observed at Concepción volcano during the inflation phase from May 5 to 14, 2010, and the deflation phase between May 24 and 31, 2010 (Fig. 2). See text for details

Table 2 Output of best fitted parameters of the open pipe model (Bonaccorso and Davis 1999) used to model the geodetic GPS deformation observed at Concepción volcano during the 2010 erupting phase

	Depth to top of magma pipe (m)	ΔP (MPa)
Inflation phase between May 5 and 14, 2010		
Average	582	25
1σ	97	11
Deflation phase between May 23 and 27, 2010		
Average	1,058	16
1σ	120	7

Input parameters are in Table 1

along a volcano conduit open at its top (i.e., Bonaccorso and Davis 1999). As magma moves upward, the walls of the conduit undergo uniform pressure change causing an outward displacement of the conduit walls, simulated by a constant cylindrical dislocation (Fig. 5). The outward displacement of the conduit walls results in the inflation of the volcano edifice and positive geodetic baseline changes. During an explosion, the pressure in the volcano conduit is reduced, causing the walls to contract inward, and hence a volcano deflation measured as a geodetic baseline contraction. The open pipe model was developed by Bonaccorso and Davis (1999), in which the upward (or downward) movement (from depth c_2 and c_1, Fig. 5) of a cylindrical magma body along a pipe of radius α embedded in a uniform elastic half-space produces a uniform dislocation of the vertical conduit walls (b), hence a given displacement of any point at the surface of the half-space. The model implies that the magma pipe does not experience any pressure change at its ends (top and bottom) representing respectively the open top and the magma source.

According to Bonaccorso and Davis (1999) and Lisowski (2007), the horizontal and vertical displacements are given by:

$$u_E = \frac{\alpha b x}{2(x^2+y^2)}\left(\frac{c_1^3}{R_1^3} - \frac{2c_1(1+\nu)}{R_1} + \frac{c_2^3(1+2\nu)+2c_2(x^2+y^2)(1+\nu)}{R_2^3}\right) \quad (1)$$

$$u_N = \frac{\alpha b y}{2(x^2+y^2)}\left(\frac{c_1^3}{R_1^3} - \frac{2c_1(1+\nu)}{R_1} + \frac{c_2^3(1+2\nu)+2c_2(x^2+y^2)(1+\nu)}{R_2^3}\right) \quad (2)$$

$$u_v = -\frac{\alpha b}{2}\left(\frac{c_1^2}{R_1^3} - \frac{2\nu}{R_1} + \frac{2\nu R_2^2 - c_2^2}{R_2^3}\right) \quad (3)$$

where u_E and u_N are the horizontal surface displacements in the easting and northing directions, respectively; u_v is the vertical surface displacement; ν is Poisson's ratio (taken to be equal to 0.25); x and y are the horizontal

Table 1 Input range of parameters used in the open pipe model (Bonaccorso and Davis 1999)

	Depth to Top of magma pipe (m)	Depth to Bottom of magma pipe (m)	Dislocation of conduit wall (m)	Radius of magma pipe (m)
Min. Val.[a]	100	2,000	0.1	5
Max. Val.[b]	1,500	2,000	70	125

[a]Minimum value

[b]Maximum value

See output of best fitted parameters in Table 2

Table 3 Summary of the results of the multivariate Ljung and Box (1978) test using the Hosking (1980) algorithm to test for whiteness at different lags in the time-series shown in Fig. 2, see also Fig. 4

TS[a] pair	p value[b]
Lag 5	
Figure 4A	0.000
Figure 4B	0.000
Figure 4C	0.000
Figure 4D	0.000
Figure 4E	0.012
Figure 4F	0.003
Lag 10	
Figure 4A	0.000
Figure 4B	0.000
Figure 4C	0.000
Figure 4D	0.001
Figure 4E	0.008
Figure 4F	0.046
Lag 15	
Figure 4A	0.000
Figure 4B	0.000
Figure 4C	0.000
Figure 4D	0.007
Figure 4E	0.025
Figure 4F	0.323
Lag 20	
Figure 4A	0.000
Figure 4B	0.000
Figure 4C	0.000
Figure 4D	0.039
Figure 4E	0.141
Figure 4F	0.543

[a]TS stands for time-series

[b]A p value < 0.01 (1 %) is an indication of significant correlation, see Hosking (1980)

coordinates of the point of interest on the ground surface relative to the deformation source location (i.e., the volcano); $R_1^2 = x^2 + y^2 + c_1^2$; and $R_2^2 = x^2 + y^2 + c_2^2$.

The conduit wall dislocation, the pipe's radius, the pressure change (ΔP) of the magma reservoir, and the shear modulus (G) are related by (Landau and Lifshitz 1986):

$$\Delta P = \frac{b}{\alpha} G \tag{4}$$

The assumption of the Earth'crust as an elastic half-space is a first-order approximation since it assumes the crust to be homogeneous and mechanically isotropic, implying a linear relationship between strain and the applied stresses (Lisowski 2007). Thus, this approximation (in particular at volcanoes) does not take into account a series of characteristics of the real crust, but it is a good approximation for deformations produced by infinitesimal and short-term phenomena on the surface or within the shallow crust (Lisowski 2007).

To estimate the baseline changes for the periods of interest (i.e., May 5 – 13 and May 23 – 29, 2010) using the open pipe model (Bonaccorso and Davis 1999), we computed first the three components of the surface displacements with Eq. (1), fixing the depth of the pipe's bottom at 2 km, compatible with the suggested depth of the shallow magma reservoir at Concepción (see later discussion). Then, we carried out a Monte Carlo simulation generating random values within the parameter space (see Table 1) and computing for each simulation the misfit of the model to the observations (baseline length variation). The best-fit parameters are summarized in Table 2. The results show that a ~400 m change of the magma pipe's top (from 1,000 to 600 m depth) can explain the observed changes in the GPS baseline length for the period of interest (Table 2).

Discussion and conclusions

The significant correlations we have found in the 2010 time series (Figs. 3 and 4) suggest that the changes in the GPS baseline, SAM daily counts, and SO_2 emissions during the eruptive phase may have shared a common source. Although the signal is weak in each time series, the cross-correlation is significant. This interpretation is reinforced by the lack of such correlations observed in the time series collected in the 2011 non-eruptive period.

The 2010 time series, however, contains a few gaps - days during which no data were collected. This is a common problem with time series generated by instruments installed on active volcanoes, and the significance of these data gaps and the interpolation methods used to fill the gaps for our interpretation warrants investigation. We found that the high cross-correlation in the 2010 time-series is insensitive to the interpolation method used. As an end member case for testing our interpolation, we replaced all the gaps in the SO_2 time series with the minimum observed values (i.e., 27 tons/day daily flux of SO_2) and recomputed the cross-correlations. Even with this extreme interpolation method, significant cross-correlation among the time series persists during the 2010 period. The main difference was a shift in the lag number of the largest significant cross-correlation (-1 instead of -3), suggesting that the -3-day lag between SO_2 emissions and GPS baseline changes may not be a very robust estimation, but again the GPS baseline changes lead SO_2 emissions (by 1 day in this case). To asses the robustness of our interpretation of the correlation among the different time series, we performed another test. Unlike the GPS baseline changes, the SAM and SO_2 values are always positive, so we also computed the cross-correlation for the 2010 data sets with the absolute value of the GPS baseline changes. Also, in this case, the cross-correlation among the different time series is still significant (although the coefficient at zero lag slightly decreases).

Given the relative short length of our time series, we further tested the robustness of the cross-correlation performing a multivariate portmanteau test as described by Hosking (1980). This test is a generalization of the univariate Ljung-Box (Q) test for white-noise in the residual of time-series (test for departure from randomness, Ljung and Box (1978)). The test can be used to test the overall randomness up to a given number of lags, instead of just testing for randomness of a particular lag (Ljung and Box 1978). The null hypothesis is that the residuals of the time series should be uncorrelated, in other words that the residuals behave like white-noise series. The residuals are defined as the difference between each element of a particular series by its mean value (Ljung and Box 1978; Hosking 1980). We applied this test to the time-series pair shown in Fig. 2 using a significance level of 1 % (Hosking 1980), and results are shown in Table 3.

Independently for the lag we performed our test (5, 10, 15, and 20 days), all the time series corresponding to the eruptive phase of 2010 do not correspond to white noise indicating the presence of non-random behavior. In contrast, the time series corresponding to the non-eruptive phase of Concepción volcano in 2011 show a much higher presence of random behavior (Table 3). If we set a higher significance level (i.e., 5 % or higher), more randomness is shown by the residuals of the 2011 time series. Even this last test supports the interpretation that the 2011 data set do not present strong correlations, while the data set corresponding to the eruptive phase of 2010 do present significant correlation at different lags, suggesting that there is a strong possibility that it is related to volcanic processes.

As the 2011 time series were gathered during the dry season, we deem that scrubbing effects of SO_2 by interactions with hydrothermal fluids are minimal, if it is taking place at all (e.g., Symonds et al. 2001). Part of the 2010 observations were made during the rainy season (May and June, Fig. 2a). However, SO_2 remains correlated with GPS baseline changes and SAM after the onset of the rainy season. Thus, if SO_2 scrubbing is taking place, it is possible that is not playing a major role in changing the SO_2 emission during our observation periods. Only a longer time series, spanning several seasonal changes, is likely to quantify how much SO_2 may be scrubbed by hydrothermal processes under Concepción.

The mild but frequent activity at Concepción volcano during the last four decades is consistent with the presence of a small-volume, shallow, and relatively open magmatic system (van Wyk de Vries 1993; Borgia et al. 2003). We were unable to gather data during the onset of the 2010 eruptive activity on March 7, but only beginning 1 month later (Fig. 2). The first set of anomalies observed between May 5 and 14, 2010 in the GPS time series (increase in baseline length of up to 12 mm), SAM daily counts (a maximum daily average increase of 89 units, 10 units lower than the maximum observed during the onset of the eruption between March 7 and 9), and SO_2 emission (a peak on the average daily flux of 643 tons/day, more than %50, Fig. 2a) can be explained by ascent of a magma column in the relatively open conduit.

Modeling results suggest that the measured 12 mm extension between the two GPS stations is consistent with the rising of a magma pipe from a depth of $\sim$1,000 to $\sim$600 m, associated with a pressure change of about 25 $\pm$ 11 MPa (assuming a rigidity of the shallow crust of 50 MPa, e.g., Chadwick et al. 1988) within the magmatic system (Table 2). Increased SO_2 emission during this period is consistent with this model, through increase exsolution of SO_2 from the ascending magma. The peak in the SAM counts during this time frame is also consistent with this model (Fig. 2).

A few days later, May 24 – 31, the descending magma column reduced the pressure in the volcano conduit, causing the walls to contract inward, which is inferred from the GPS data as a volcano deflation (about 17 mm shortening of the GPS baseline, Fig. 2). This deflation was accompanied by an increase of the daily SAM counts of $\sim$80 units. No anomalous SO_2 emission was observed during this period (fluxes $<$ 200 tons/day), consistent with the model of magma deepening. The modeling suggests that for this event, the top of the magma column descended to a depth of about 1000 m, approximately sea-level. This event was associated with the end of the volcanic crisis.

We choose the base (bottom) of the magma pipe to be at 2,000 m depth for two main reasons. First, this almost is the mean depth ($\sim$1.7 – 2.1 km depth) of the center of a density anomaly below Concepción volcano derived from an 3-D inversion of gravity data (Saballos 2013), which may be associated with a shallow magmatic reservoir. Second, based on published data, Borgia and van Wyk de Vries (2003 and references therein) proposed the existence of density and rheological discontinuities below Concepción volcano at about 2,000 m depth, favoring the formation of a magmatic reservoir at this depth.

Both GPS stations (CON1 and SINT, Fig. 1) used in this study are located a few meters above sea level $\sim$162 and $\sim$260 m, respectively, compared to the volcano's summit elevation $\sim$1600 m. Thus, topography will not impact the results of our modeling in a significant way since the uncertainties of the model results are of the same order of the average GPS elevation. Williams and Wadge (1998) suggest to use the topographic elevation of the observation point to compute a first order correction due to the presence of the volcanic edifice. Following their suggestion, we can apply a constant correction of ∼200 m to the depth of the estimated top and bottom of the magma pipe. However, it is worth noting that the shallower the source, the greater the effect of the topography on the model results. Given a magmatic source ∼2 km depth (Saballos 2013), the effects are not significant. Given the small geodetic network utilized in this study, other source models could fit the data equally well. Still the known behavior of Concepción as an open conduit volcano (van Wyk de Vries 1993; Borgia et al. 2003; Saballos et al. 2013) suggests the Bonaccorso and Davis (1999) model as the most physically reasonable model to apply.

Even with the lack of the seismic waveform data during the periods of interest (thus restricted to changes in SAM values, and what is reported in the INETER's monthly bulletins), we have shown that a simple cross-correlation analysis with basic geophysical data can furnish valuable information of the dynamics of Concepción volcano. Overall, these results suggest that much can be gained through a more robust multidisciplinary approach (i.e., the gathering of continuous geophysical data on dense networks), although we note that the comparatively small dimension of Ometepe Island imposes some constraints on spatial coverage of these networks. Such a network would, in turn, furnish vital information (e.g., magma intrusion linked to enhanced unrest visible at the surface and retreat of magma linked to waning or end of volcanic activity) to decision–makers during volcanic crises. Because the magmatic system of Concepción volcano is relatively open and of small-volume, a single data set may not provide enough information to understand the processes taking place during volcanic activity, and some important details of the system dynamics may be overlooked.

Acknowledgments Research of J. A. Saballos was provided by the Geology Department and the Institute for the Study of the Latin America and the Caribbean of the University of South Florida. Research of V. Conde has been provided by the Swedish International Development Cooperation Agency (SIDA). We also want to acknowledge the Instituto Nicaragüense de Estudios Territoriales for providing the SAM data and logistic support. UNAVCO provided GPS equipment for several campaigns. The authors thank Sarah Kruse, Diana Roman, Tim Dixon, Paul Wetmore, and Peter La Femina, who all provided valuable guidance during the project. We are grateful for thorough reviews by two anonymous reviewers, which greatly improved the manuscript.

References

Altamimi Z, Collilieux X, Métivier L (2011) ITRF2008: an improved solution of the international terrestrial reference frame. J Geodesy 85:457–473. doi:10.1007/s00190–011–0444–4

Bonaccorso A, Davis P (1999) Models of ground deformation from vertical volcanic conduits with application to eruptions of Mount St. J Geophys Res 104(B5):10–531

Borgia A, Wyk van, de Vries B (2003) The volcano-tectonic evolution of Concepción, Nicaragua. Bull Volcanol 65:248–266

Casadevall TJ, Johnston DA, Harris DM, Rose WI, Malinconico LL, Stoiber RE, Bornhorst TJ, Williams SN, Woodruff L, Thompson J (1981) SO_2 emission rates at Mt. St. Helens from March 29 through December, 1980. In: Lipman PW, Mullineaux DR (eds) The 1980 eruption of Mt. St. Helens, Washington, US Geological Survey Profesional Paper 1250. USA, pp 193–207

Chadwick WW, Archuleta RJ, Swanson DA (1988) The mechanics of ground deformation precursory to dome-building extrusions at Mount St. Helens 1981–1982. J Geophys Res 93(B5):4351–4366

Chatfield C (1996) The analysis of time–series: an introduction, 5th edn. Chapmann & Hall/CRC, Florida

Dalton MP, Waite GP, Watson IM, Nadeau PA (2010) Multiparameter quantification of gas release during weak Strombolian eruptions at Pacaya Volcano, Guatemala. Geophys Res Lett 37(L09303). doi:10.1029/2010GL042,617

Endo ET, Murray T (1991) Real–time seismic amplitude measurement (RSAM): a volcano monitoring and prediction tool. Bull Volcanol 53:533–545

Fischer TP, Roggensack K, Kyle PR (2002) Open and almost shut case for explosive eruptions; vent processes determined by SO_2 emission rates at Karymsky Volcano, Kamchatka. Geology 30:1059–1062

Galle B, Oppenheimer C, Geyer A, McGonigle AJ, Edmonds M, Horrocks L (2003) A miniaturised ultraviolet spectrometer for remote sensing of SO_2 fluxes: a new tool for volcano surveillance. J Volcanol Geotherm Res 119(14):241–254. doi:10.1016/S0377-0273(02)00356-6

Galle B, Johansson M, Rivera C, Zhang Y, Kihlman M, Kern C, Lehmann T, Platt U, Arellano S, Hidalgo S (2010) Network for observation of volcanic and atmospheric change (NOVAC)–a global network for volcanic gas monitoring: Network layout and instrument description. J Geophys Res 115(D05304). doi:10.1029/2009JD011,823

Gottsmann J, Carniel R, Coppo N, Wooller L, Hautmann S, Rymer H (2007) Oscillations in hydrothermal systems as a source of periodic unrest at caldera volcanoes: Multiparameter insights from Nisyros, Greece. Geophys Res Lett 34(L07307). doi:10.1029/2007GL029,594

Hill BE, Connor CB, Jarzemba MS, LaFemina PC, Navarro M, Strauch W (1998) 1995 eruptions of Cerro Negro volcano, Nicaragua, and risk assessment for future eruptions. Geol Soc Am Bull 110:1231–1241

Hosking JR (1980) The multivariate portmanteau statistic. J Am Stat Assoc 75(371):602–608

Ichihara M, Takeo M, Yokoo A, Oikawa J, Ohminato T (2012) Monitoring volcanic activity using correlation patterns between infrasound and ground motion. Geophys Res Lett 39(4). doi:10.1029/2011GL050,542

INETER (2008) Boletín mensual: Sismos y Volcanes de Nicaragua, Octubre, 2008. Managua. http://webserver2.ineter.gob.ni/geofisica/boletin/2008/10/index0810.htm

INETER (2010a) Boletín mensual: Sismos y Volcanes de Nicaragua, Abril, 2010. Managua. http://webserver2.ineter.gob.ni/geofisica/boletin/2010/04/index1004.htm

INETER (2010b) Boletín mensual: Sismos y Volcanes de Nicaragua, March, 2010. Managua. http://webserver2.ineter.gob.ni/geofisica/boletin/2010/03/index1003.htm

INIFOM (2001) Caracterizaciones Municipales de Nicaragua. Technical report. Instituto Nicaragënse de Fomento Municipal, available at http://www.inifom.gob.ni/municipios/municipios.html

Kazahaya R, Mori T, Takeo M, Ohminato T, Urabe T, Maeda Y (2011) Relation between single very-long-period pulses and volcanic gas emissions at Mt. Asama, Japan. Geophys Res Lett 38(L11307). doi:10.1029/2011GL047,555

Kutterolf S, Freundt A, Peréz W, amd U Schacht TM, Wehrmann H, Schmincke HU (2008) Pacific offshore record of plinian arc volcanism in Central America: 1. along-arc correlations. Geochem Geophys Geosyst 9:Q02S01. doi:10.1029/2007GC001,631

Landau LD, Lifshitz EM (1986) Theory of elasticity: Course of theoretical physics, 3rd edn, vol 7. Pergamon Press, Oxford

Lisowski M (2007) Analytical volcano deformation source models. In: Dzurisin D (ed) Volcano deformation: geodetic monitoring techniques. Praxis Publishing Ltd, Chichester, pp 279–304

Ljung GM, Box GE (1978) On a measure of lack of fit in time series models. Biometrika 65(2):297–303

McBirney A, Williams H (1965) Volcanic history of Nicaragua. University of California Publications in Geological Sciences 55:1–65

McGee KA, Sutton AJ (1994) Eruptive activity at Mount St Helens, Washington, USA, 1984-1988: a gas geochemestry perspective. Bullet Volcanol 56:435–446

Nadeau PA, Palma JL, Waite GP (2011) Linking volcanic tremor, degassing, and eruption dynamics via so_2 imaging. Geophys Res Lett 38(L01304). doi:10.1029/2010GL045,820

Nishimura T (2009) Ground deformation caused by magma ascent in an open conduit. J Volcanol Geotherm Res 187(3):178–192

Olmos R, Barrancos J, Rivera C, Barahona F, López D, Henriquez B, Hernández A, Benitez E, Hernández P, Pérez N, Galle B (2007) Anomalous emissions of SO_2 during the recent eruption of Santa Ana Volcano, El Salvador, Central America. Pure Appl Geophys 164:2489–2506. doi:10.1007/s00024-007-0276-6

Platt U, Stutz J (2008) Differential optical absorption spectroscopy: Principles and applications, 1st edn. Springer-Verlag Berlin, Heidelberg, Germany

Saballos JA (2013) Short and long term volcano instability studies at concepción volcano, Nicaragua. Ph.d. dissertation, University of South Florida, Tampa

Saballos JA, Malservisi R, Connor C, Femina PL, Wetmore P (2013) Gravity and geodesy at Concepción volcano, Nicaragua. In: Rose W, Palma JL, Granados HD, Varley N (eds) Understanding open–vent volcanism and related hazards. Geological Society of America Special Paper 498

Siebert L, Simkin T, Kimberly P (2011) Volcanoes of the World, 3rd edn. University of California Press, Berkeley

Symonds R, Gerlach T, Reed M (2001) Magmatic gas scrubbing: implications for volcano monitoring. J Volcanol Geotherm Res 108(1–4):303–341

Voight B, Sparks RSJ, Miller AD, Stewart RC, Hoblitt RP, Clarke A, Ewart J, Aspinall WP, Baptie B, Calder ES, Cole P, Druitt TH, Hartford C, Herd RA, Jackson P, Lejeune AM, Lockhart AB, Loughlin SC, Luckett R, Lynch L, Norton GE, Robertson R, Watson IM, Watts R, Young SR (1999) Magma flow instability and cyclic activity at Soufrière Hills Volcano, Montserrat, British West Indies. Science 283(5405):1138–1142. doi:10.1126/science.283.5405.1138

van Wyk de Vries B (1993) Tectonics and magma evolution of Nicaraguan volcanic systems. Ph.d. dissertation, Open University, Milton Keynes

Watson I, Oppenheimer C, Voight B, Francis P, Clarke A, Stix J, Miller A, Pyle D, Burton M, Young S, Norton G, Loughlin S, Darroux B (2000) The relationship between degassing and ground deformation at Soufrière Hills Volcano, Montserrat. J Volcanol Geotherm Res 98(1–4):117–126. doi:10.1016/S0377-0273(99)00187-0

Williams CA, Wadge G (1998) The effects of topography on magma chamber deformation models: Application to Mt. Etna and radar interferometry. Geophys Res Lett 25(10):1549–1552

Williams-Jones G, Stix J, Heiligmann M, Barquero J, Fernández E, González E (2001) A model of degassing and seismicity at Arenal Volcano, Costa Rica. J Volcanol Geotherm Res 108(1–4):121–139